JOURNAL OF GEOPHYSICAL RESEARCH, VOL. 115, A04302, doi:10.1029/2009JA014922, 2010

Large-scale traveling ionospheric disturbances impacting equatorial ionization anomaly development in the local morning hours of the Halloween Superstorms on 29–30 October 2003

Ildiko Horvath[1,2] and Brian C. Lovell[1,2]

Received 23 September 2009; revised 27 October 2009; accepted 3 November 2009; published 1 April 2010.

[1] This study investigates the development of EIA-like features during the Halloween Superstorms. These features are similar to a well-developed equatorial ionospheric anomaly (EIA) and therefore suggest superfountain effects. We tracked EIA-like features in the early-morning sector of 29–30 October 2003 and at around midday on 30 October. Their plasma environment was studied with field-aligned plasma density, vertical plasma drift, electron temperature, and vertical plasma flow profiles. Coupled thermosphere-ionosphere plasmasphere (CTIP) simulations reproduced storm-generated equatorward wind surges. When these EIA-like features appeared early morning on 29–30 October, there was no forward fountain circulation; only large-scale traveling ionospheric disturbances (TIDs) and strong equatorward winds were present. These provide observational evidence that large-scale TIDs created large plasma depletions over the dip equator and with the aid of equatorward winds some large enhancements at ~±30°N (geomagnetic), resulting in the development of early-morning EIA-like features. We identified TID signatures in the equatorial and midlatitude ionosonde and magnetometer data, and studied EIA-like features at around midday on 30 October utilizing non-field-aligned TOPEX TEC (2000 UT) and published CHAMP TEC (2030 UT; 2200 UT) line plots. According to our analysis, the EIA-like features seen in the TEC data were created by large-scale TIDs at 2000 and 2030 UT and by the combined effects of large-scale TIDs and forward superfountain at 2200 UT. CTIP simulations demonstrate the crucial role of the neutral winds' mechanical or direct effects in the development of high plasma densities at low midlatitudes.

Citation: Horvath, I., and B. C. Lovell (2010), Large-scale traveling ionospheric disturbances impacting equatorial ionization anomaly development in the local morning hours of the Halloween Superstorms on 29–30 October 2003, *J. Geophys. Res.*, *115*, A04302, doi:10.1029/2009JA014922.

1. Introduction

[2] At low mid- and midlatitudes, positive storm effects are due to the mixture of prompt penetrating eastward **E**-field (i.e., solar wind induced **E**-field that penetrates into the magnetic equator [*Mannucci et al.*, 2005; *Tsurutani et al.*, 2005, 2008]) and direct storm-time equatorward winds [*Balan et al.*, 2009]. Prompt penetrating eastward **E**-field drives a superfountain and thus creates a large equatorial anomaly with large plasma enhancements at midlatitudes due to the substantial uplift of the equatorial and midlatitude ionosphere to greater heights [*Tsurutani et al.*, 2004]. Meanwhile, the direct effects of strong equatorward neutral winds are crucial to raise the ionosphere at low midlatitudes to high altitudes where the recombination rates are low [*Balan et al.*, 2009]. However, dawn-dusk interplanetary **E**-fields have other significant effects, which create strong ring currents when the energy and momentum input into the high-latitude ionosphere maximizes [*Tsurutani et al.*, 2004, 2008]. Furthermore, electric current variations set up mechanisms producing the Lorenz force and Joule heating that launch atmospheric gravity waves (AGWs) and traveling ionospheric disturbances (TIDs [*Hunsucker*, 1982]).

[3] Soon after the start of the Halloween Superstorms, some large-scale TIDs were generated in the auroral zone on 29 October 2003 that traveled with a period of 40–60 min equatorward as large-scale solitary type waves in different longitude sectors [*Perevalova et al.*, 2008; *Afraimovich et al.*, 2005, 2008]. The resultant plasma density perturbations were mapped over North America by *Ding et al.* [2007] and their parameters were defined by *Perevalova et al.* [2008]. Meanwhile, the equatorial ionization anomaly (EIA) also displayed some unusual behavior. It developed at an unusually early time, in the morning sector, over Brazil and the Atlantic after the electric (**E**) field polarity reversal

[1]Security and Surveillance, School of Information Technology and Electrical Engineering, University of Queensland, Brisbane, Queensland, Australia.
[2]National ICT Australia (NICTA), Queensland Research Laboratory, Brisbane, Qld, Australia.

0148-0227/10/2009JA014922

Table 1. List of Ground-Based Ionosonde and Magnetometer Observatory Sites Providing Data for This Study and Their Geographic Locations and Geomagnetic Latitudes

Station Name[a]	Geographic		Geomagnetic
	Latitude (°N)	Longitude (°E)	Latitude (°N)
Ascension Island (I,M)	−7.95	345.62	−2.36
Athens (I)	23.50	38.00	19.70
Bangui (M)	4.33	18.57	4.20
Bay St Luis (I,M)	30.35	270.37	40.05
Chichijima (M)	27.10	142.18	18.47
Dyess (I)	32.40	260.30	41.31
Guam (M)	13.59	144.87	5.30
Honolulu (M)	21.32	201.94	21.83
Huancayo (M)	−12.04	284.68	−1.80
Jicamarca (I,M)	−12.10	283.00	−1.89
M'Bour (M)	14.38	343.03	20.11
Osan (I,M)	37.1	127.00	27.33
Papeete (M)	−17.6	210.4	−15.17
Puerto Rico (I)	18.5	292.80	28.72
San Juan (M)	18.11	293.15	28.31
San Pablo-Toledo (M)	39.55	355.65	42.78
Tsumeb (M)	−19.20	17.58	−18.77
Tucuman (I)	−26.9	294.60	−16.7

[a]I, ionosonde; M, magnetometer.

[*Batista et al.*, 2006]. On 30 October 2003, the daytime EIA largely intensified at around midday over the Eastern Pacific [*Mannucci et al.*, 2005] due to some prompt penetration **E**-fields [*Tsurutani et al.*, 2005] and strong equatorward neutral winds [*Balan et al.*, 2009].

[4] Although the superfountain effects have been extensively investigated by many studies [e.g., *Mannucci et al.*, 2005; *Tsurutani et al.*, 2004, 2008], the impact of large-scale TIDs on superfountain effects received little attention and thus such impact is still unclear. We still do not know how the simultaneously occurring large-scale TIDs affected the EIA and contributed to its unusual behavior. This study aims to investigate in detail the EIA's early-morning development over Brazil and the Atlantic, and the intensification of daytime EIA over the Eastern Pacific. Our main goal is to find out the impact of equatorward propagating large-scale TIDs on the EIA early morning and at around midday.

2. Data Sets and Methodology

[5] For tracking plasma density features and their plasma environment, we utilized the multi-instrument in situ measurements of the Defense Meteorological Satellite Program (DMSP; see details in the work of *Horvath* [2007] and *Horvath and Lovell* [2009]). Collected along the descending passes of flights 13, 14, and 15 (indicated as F13, F14, and F15) at ~850 km altitude during the period of 28–31 October 2003, plasma density (Ni, i^+/cm^3), electron temperature (T_e, K), vertical drift velocity (V_Z; m/s), and vertical plasma flux [F_Z; $i^+/(cm^2\ s)$] values were employed. For obtaining over-the-ocean total electron content (TEC; TECU) values at ~1336 km altitude, radar altimeter sea surface height measurements of the TOPEX/Poseidon mission (see details in the work of *Horvath* [2006]) collected during cycles 409 and 410 were utilized. We gave preference to field-aligned passes as those provide true plasma density profiles [*Horvath and Lovell*, 2009]. Neutral wind simulations were provided by the coupled thermosphere-ionosphere plasmasphere (CTIP) model [*Fuller-Rowell et al.*, 1996] and allowed us to observe global wind pattern variations.

[6] Various ionospheric parameters such as foF2 (MHz) representing F2-layer critical frequency and hmF2 (km) indicating maximum F2 layer height were provided by 15 min ionosonde data from various low-latitude and midlatitude stations (see Table 1). Since the critical frequency is proportional to the square root of the peak electron density, we computed and utilized $\{[foF2]^2; \text{in } MHz^2\}$ values in order to observe peak electron density variations.

[7] For studying the 29–30 October 2003 Halloween Superstorms, the interplanetary magnetic field (IMF) vectors ($\mathbf{B_X}$, $\mathbf{B_Y}$, $\mathbf{B_Z}$; nT) and proton speed (V_P; km/s) values measured by the ACE satellite (see details in the work of *Horvath and Lovell* [2008]) and various geomagnetic indices (*Dst* (nT), AE (nT), Kp) were utilized.

[8] $\mathbf{E} \times \mathbf{B}$ drift/zonal **E**-field estimations [*Anderson et al.*, 2002] were obtained by computing ΔH ($H_{equ} - H_{non\text{-}equ}$; nT) values for four longitude sectors. These are the (1) African (~18°E; geographic), (2) Australian (~145°E), (3) American (~290°E), and (4) Atlantic (~345°E) sectors. The station pairs of (1) Tsumeb-Bangui, (2) Guam-Chichijima, (3) Huancayo-San Juan, and (4) Ascension Island-M'Bour, respectively, provided the data (see Table 1). We also computed F (nT) component values (see more details in section 3.2) in order to observe total magnetic **B**-field variations.

3. Observational Results and Interpretations

3.1. 29–30 October 2003 Halloween Superstorms

[9] The Halloween Superstorms are a series of three storms occurring between 29 and 31 October 2003. As shown in Figure 1, the IMF $\mathbf{B_Z}$ component turned southward three times and each time the ring current intensified. The *Dst* index reached a local minimum of −180 nT at 1000 UT on 29 October when an intense sub-storm occurred. There were two more intensifications, −363 nT at 0100 UT and −401 nT at ~2259 UT, on 30 October. These registered two superstorms and their sudden commencements (SSC1 and SSC2) were triggered by fast coronal mass ejections [*Zurbuchen et al.*, 2004; *Tsurutani et al.*, 2005]. Their impacts created sharp solar wind increases on 29 October (from 782 to 1810 (km/s)) and on 30 October (from 964 to 1760 (km/s)). SSC1 occurred on 29 October at 0611 UT when the AE index suddenly increased to 4056 nT (Kp ~ 9). SSC2 was seen on 30 October at 1627 UT when the AE index sharply increased to 2976 nT (Kp ~ 9). Their respective recovery phases started at ~0100 UT on 29 October (R1) and at 2259 UT 30 October (R2) [*Ding et al.*, 2007]. According to the study of *Ding et al.* [2007], the occurrence of large-scale TIDs coincided with these two SSCs.

[10] Figure 2 shows the locations of magnetometer stations providing data and the ΔH variations during the Halloween Superstorms. Largest ΔH variations (between 500 and −250 nT) occurred over Huancayo that is close to the center of the South Atlantic Magnetic Anomaly (SAMA). $\mathbf{E} \times \mathbf{B}$ drifts are modeled as $\mathbf{E} \times \mathbf{B}/B^2$ [*Kendall and Pickering*, 1967]. $\mathbf{E} \times \mathbf{B}$ drift variations in the SAMA region are due to the modified ionospheric conductivity distribution increasing the **E**-field and to the weak **B**-field

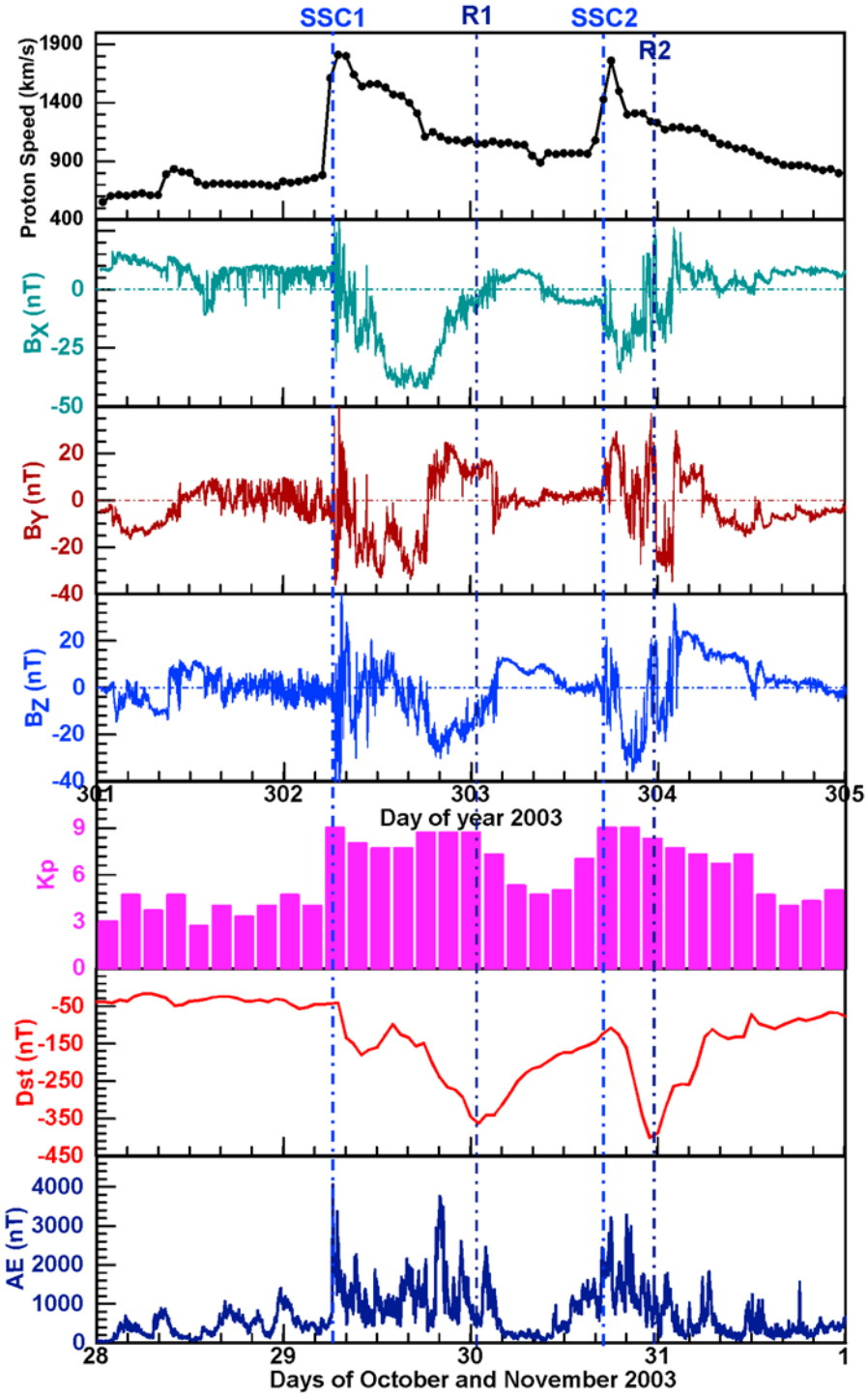

Figure 1. The nature of the Halloween Superstorm is illustrated by the ACE interplanetary plasma and magnetic field measurements and by the Kp, *Dst*, and AE geomagnetic indices. Two shock impacts resulted in two sudden storm commencements: SSC1 and SSC2. Recovery phases are indicated as R1 and R2.

[*Abdu*, 1997; *Abdu et al.*, 2005; *Basu et al.*, 2001, 2007]. Away from the SAMA center (such as over Ascension Island, Bangui, and Guam) the smaller ΔH variations indicate smaller $\mathbf{E} \times \mathbf{B}$ drift variations that are due to the weaker **E**-field and stronger **B**-field.

3.2. Development of an EIA-like Feature in the Local Morning Sector (0800–1130 UT) on 29 October in the African Sector and Over the Atlantic

[11] In Figure 3 (top), the DMSP F14 and F15 Ni line-maps show the morning ionosphere between 0630 and

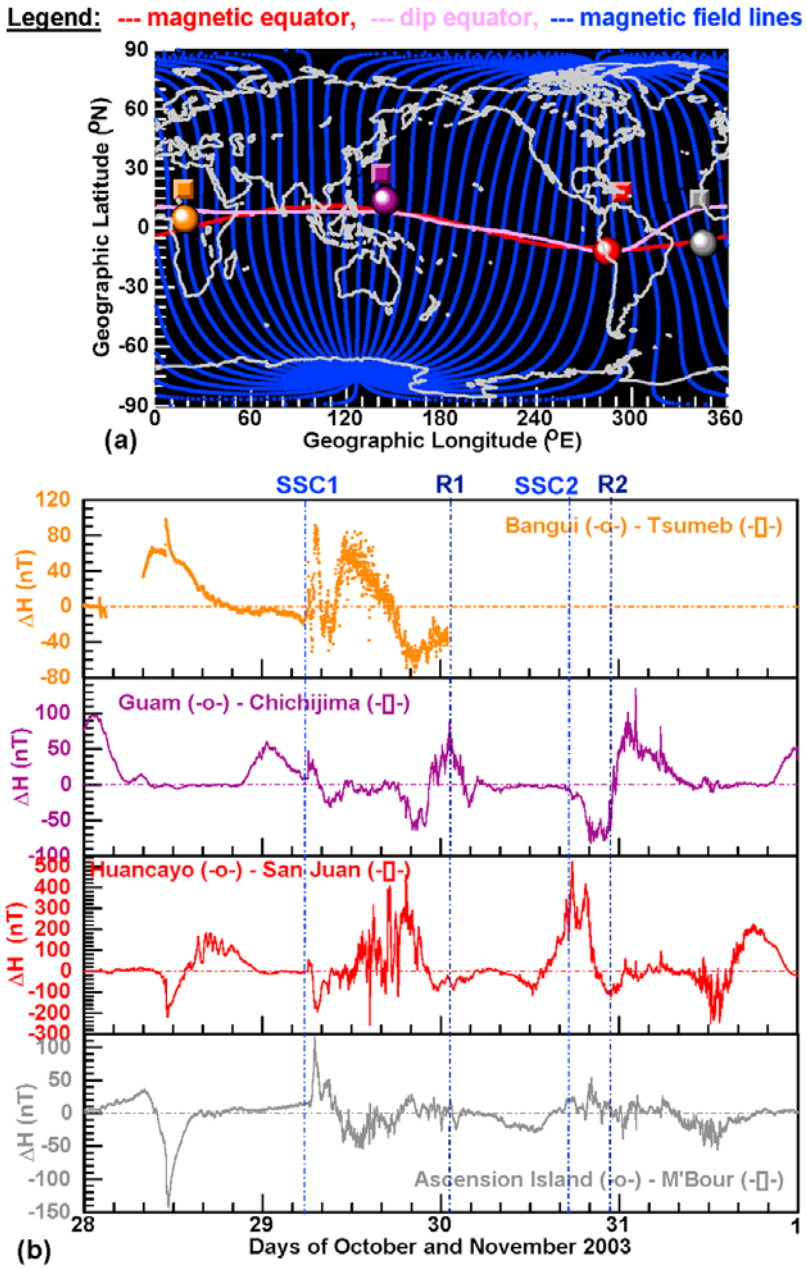

Figure 2. The global map (a) depicts the ground-based magnetometer stations providing data for the ΔH line plots (b) for the chosen longitude sectors.

1500 UT. The DMSP data recording is such that UT varies with longitude, in this case along the descending passes (see details in the work of *Horvath* [2007]). These F14 and F15 maps tracked low-latitude and midlatitudes at 0800 and 0930 LT, respectively. They depict the sudden intensification of low-latitude and midlatitude plasma densities in the early-morning hours of 29 October, soon after SSC1 (0611 UT), in the vicinity of the American continents and over Africa. This interesting phenomenon of the Halloween Superstorms was investigated in detail by *Batista et al.* [2006] in the American sector and was interpreted as the sudden intensification of the EIA.

[12] In Figure 3 (middle), the Ni-Te line plot pairs show some of the F15 passes in latitudes in order to further demonstrate the sudden intensification of low-latitude and midlatitude plasma densities at ~0930 LT and different UT. These line plots are not field-aligned and therefore cannot provide true cross sections. However, pass 5 still clearly illustrate the sudden development of a symmetrical EIA-like feature in the African sector when the high-latitude ion temperatures suddenly increased from ~5000 K (see pass 4) to ~6000–6400 K (see pass 5). This sudden Te increase indicates the presence of large equatorward wind surges (see CTIP simulations and more details below). In good agreement with the 1000–1100 UT GPS TEC map of *Batista et al.* [2006], pass 7 at ~1130 UT shows the undulating high plasma densities at southern low-latitude and midlatitudes,

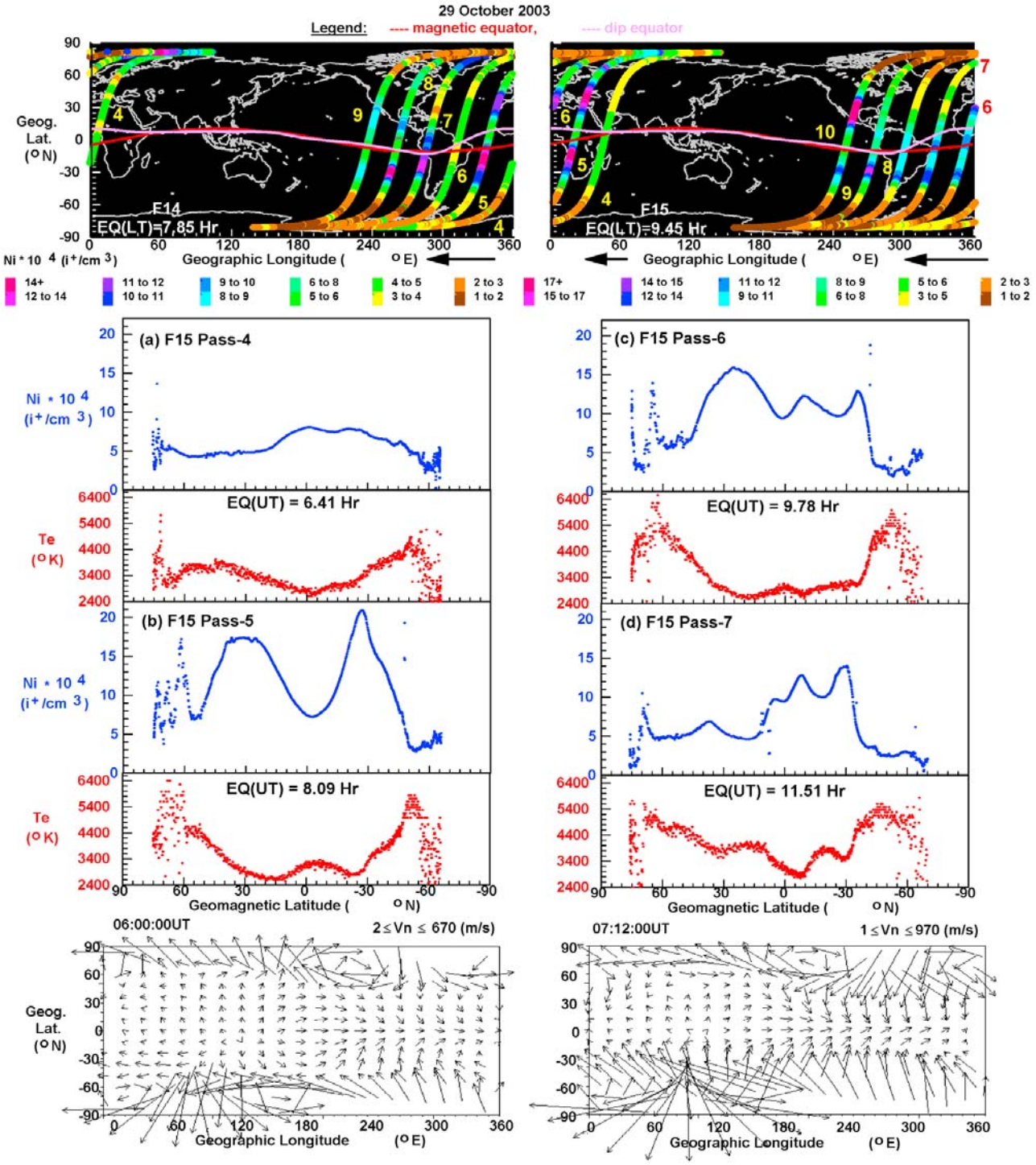

Figure 3. Two DMSP Ni line maps and four Ni-Te line plot pairs illustrate the sudden development of EIA-like features in the local early-morning sector of 29 October 2003 over the African continent and the Atlantic. CTIP modeled strong equatorward wind surges there and thus illustrate the relative importance of direct wind effects in maintaining high plasma densities at midlatitudes.

close to the Brazilian sector, while Ti remained elevated (~5800 K) at high latitudes.

[13] In Figure 3 (bottom), two CTIP vector maps, modeled for 0600 and 0712 UT, illustrate how the neutral winds varied globally at 300 km altitude before and after SSC1, respectively. The sudden intensification of equatorward neutral winds in the African sector where this EIA-like feature was detected by pass 5 and over the Eastern Pacific and the Atlantic is evident. Thus, these storm-generated equatorward winds significantly contributed to the devel-

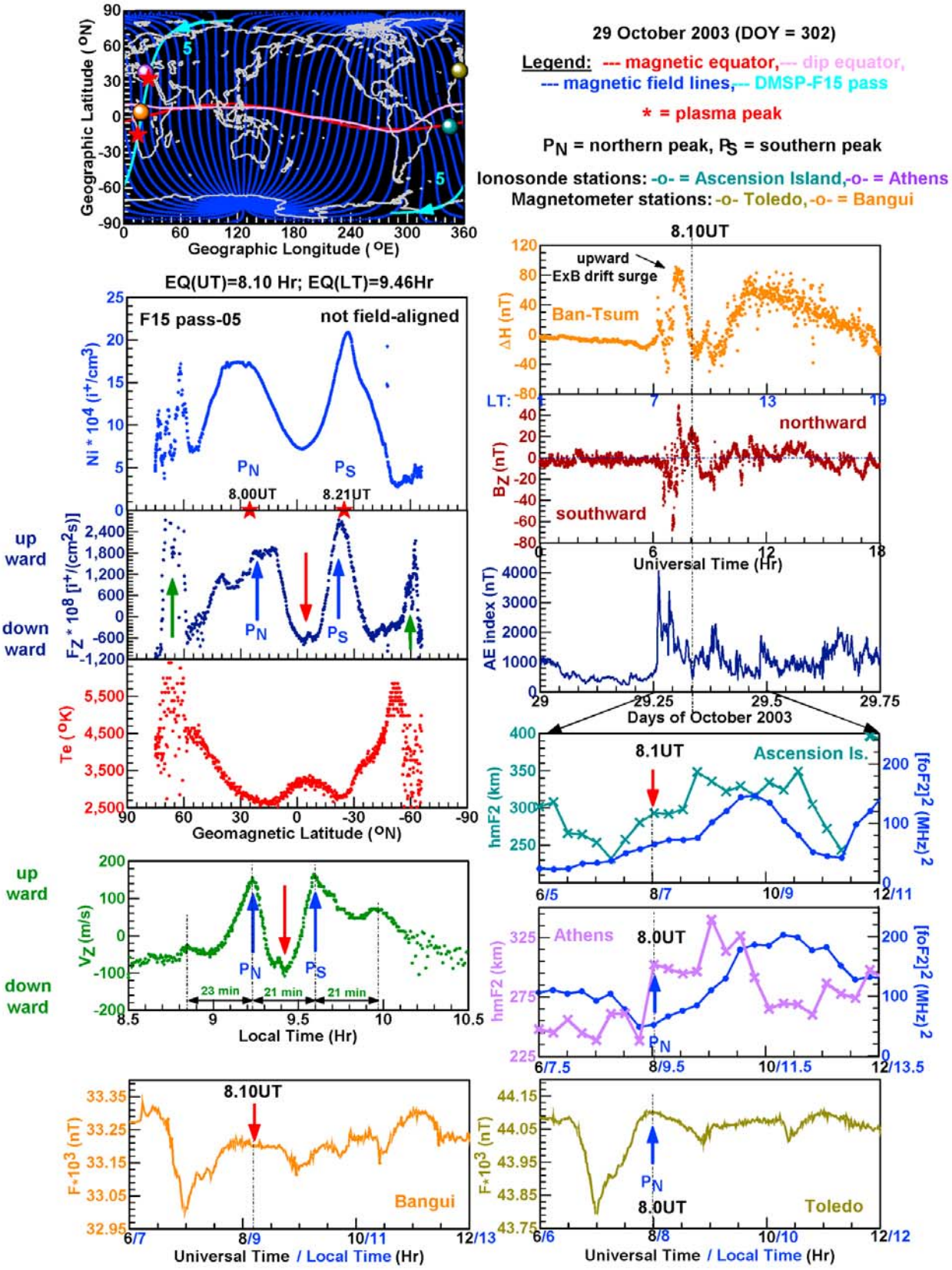

Figure 4. The global map shows the ground track of F15 pass 05, and the locations of local ionosonde and magnetometer stations. The various line plots tracked large-scale TIDs and their signatures in the early-morning hours (~0800 UT) of 29 October 2003.

opment of this EIA-like feature and to the undulating high plasma densities at southern low-latitude and midlatitudes close to the Brazilian sector.

[14] Figure 4 is constructed to unravel the development of this EIA-like feature tracked by the not field-aligned F15 pass 5 (see map). Its crest-like features, called peaks, are situated at around ±30°N (geomagnetic) indicating superfountain effects [*Tsurutani et al.*, 2004; *Mannucci et al.*, 2005; *Balan et al.*, 2009]. Thus, if this double-peak structure was an equatorial anomaly, we expect to see an intensified forward plasma fountain (i.e., superfountain) circulation in the F_Z data. This is characterized by an $\mathbf{E} \times \mathbf{B}$ driven upward flow over the equator, and by downward flows at the crests driven by gravity and pressure gradient forces (see details in the work of *Horvath and Lovell* [2008]).

[15] As the Ni-F_Z line plots shows, there is a large downward plasma flow (see red arrow) over the different equators that created a large depletion, and a large upward flow (see blue arrows) at each peak that formed each plasma peak. These Ni and F_Z line plots indicate the absence of forward fountain circulation described above, and thus provide observational evidence that this EIA-like feature was not created by a forward superfountain. Therefore it is not an equatorial anomaly. The F_Z plot also tracked large upward plasma flows at auroral latitudes (see green arrows). In latitude, the entire F_Z plot shows the periodic variation of upward and downward plasma flows forming a regular pattern. At auroral latitudes, the Te line plot tracked peak electron temperatures (~5700 K). These indicate that large amounts of energy became deposited into the auroral region, which heated the thermosphere and drove equatorward wind surges [*Rishbeth et al.*, 1987; *Prolss*, 1987] that were successfully modeled by CTIP (see Figure 3). Shown by the Ni and F_Z plots, these strong wind surges caused upwellings at northern high latitudes (see green arrows).

[16] In order to find out the origin of these underlying vertical upward and downward drifts, the vertical drift (V_Z) data were analyzed. Plotted against LT, the V_Z line plot shows the periodic variation (~21 min; measured in LT) of V_Z. Characteristic to large-scale TIDs, the cycles cover thousands of kilometers. The V_Z plot tracked some large positive (see blue arrows) and negative (see red arrow) amplitudes around the dip equator, and thus reveals that the large-scale TID-related vertical upward and downward drifts created this EIA-like feature.

[17] This EIA-like feature's trough developed over Bangui (see map). Thus, the local (Bangui-Tsumeb) ΔH line plot gives an accurate estimation of the local $\mathbf{E} \times \mathbf{B}$ variation. Meanwhile, the accompanying $\mathbf{B_Z}$ and AE plots illustrate the underlying IMF and auroral variations. At 0611 UT, the first southward turning of $\mathbf{B_Z}$ reaching −70 nT caused a prompt AE intensification and a *Dst* increase indicating SSC1. There was also an upward $\mathbf{E} \times \mathbf{B}$ drift surge then. All these indicate the prompt penetration of an eastward magnetospheric **E**-field from high to low latitudes [*Sahai et al.*, 2005; *Abdu et al.*, 2008]. This EIA-like feature was detected two UT hours later (0800 UT). Before and after this upward $\mathbf{E} \times \mathbf{B}$ drift surge, there were $\mathbf{E} \times \mathbf{B}$ drift fluctuations triggered by high-latitude energy injections as indicated by the sudden AE increases. Such energy inputs have the ability to launch large-scale TIDs [*Hunsucker*, 1982; *Hocke and Schlegel*, 1996].

[18] In order to identify the signatures of these TID-related vertical upward and downward drifts in the local ionosonde data, we utilized $[foF2]^2$ and hmF2 measurements from Athens and Ascension Island (see map). This EIA-like feature's northern peak developed over Athens, and Ascension Island was the nearest equatorial ionosonde station (see map). At the dip equator, the hmF2 values were kept constant at ~290 km when this strong equatorial downward drift was observed (0800–0830 UT) and thus indicates that the strong TID-related downward drift stopped any F2-layer rising, which in turn damped the increase of plasma density. Over Athens, there was a sudden increase in hmF2 from 235 km to 300 km that onset an $[foF2]^2$ increase indicating the action of a strong TID-related upward drift at the northern peak. The enhanced equatorward directed meriodional winds, generated by wind surges due to auroral heating (see CTIP simulations in Figure 3), also contributed to this strong height increase at the plasma peak and prevented plasma loss so plasma could accumulate [*Balan et al.*, 2009].

[19] For investigating the total magnetic **B**-field (F) variation at the equatorial trough and northern peak, the Bangui and Toledo F-component magnetometer data, respectively, were utilized (see map). These allowed us to identify TID-related vertical upward and downward drift signatures in the F data. Over Bangui, where the downward drift occurred, the *F* values were suppressed. Oppositely, over Toledo, where the upward drift took place, there was a substantial total field increase. *Ding et al.* [2007] traced the **B**-field variations back to the variations of the X-component indicating electric current (**J**) variations. Such **J** and thus total **B**-field variations launch AGWs and TIDs through mechanisms involving the Lorenz force ($\mathbf{J} \times \mathbf{B}$) and Joule heating ($\mathbf{J} \times \mathbf{E}$) [*Hunsucker*, 1982].

3.3. Development of an EIA-Like Feature in the Local Morning Sector (1630 UT) on 29 October Over the Eastern Pacific

[20] According to the F15 pass 10 (see F15 map in Figure 3), there was another plasma density intensification at low midlatitudes in the early-morning hours (~0930 LT) of 29 October over the Eastern Pacific at ~1630 UT. Figure 5 is constructed to study this event with a mostly field-aligned detection. This pass is exactly field-aligned between the two peaks (see global maps and pink trace) where it reveals the real shape of this EIA-like feature. Its most distinctive characteristic is a broad equatorial trough. Although this pass is almost field-aligned at higher latitudes, it does not show the exact cross sections of the peaks. Meanwhile, the F_Z line plot tracked the underlying plasma circulation. As before (0800 UT; see Figure 4), it is characterized by a large downward plasma flow (see red arrow) over the equator and large upward plasma flows (see blue arrows) at the plasma peaks. This almost field-aligned F_Z plot tracked large upward plasma flows at auroral latitudes (see green arrows) where T_e peaked (~6000 K) and the traveling of this perturbation toward the equator. By plotting the V_Z values against the local time, the presence of large-scale TIDs (~15 min in LT) became more obvious. These Ni, F_Z, and V_Z line plots provide observational evidence that just like

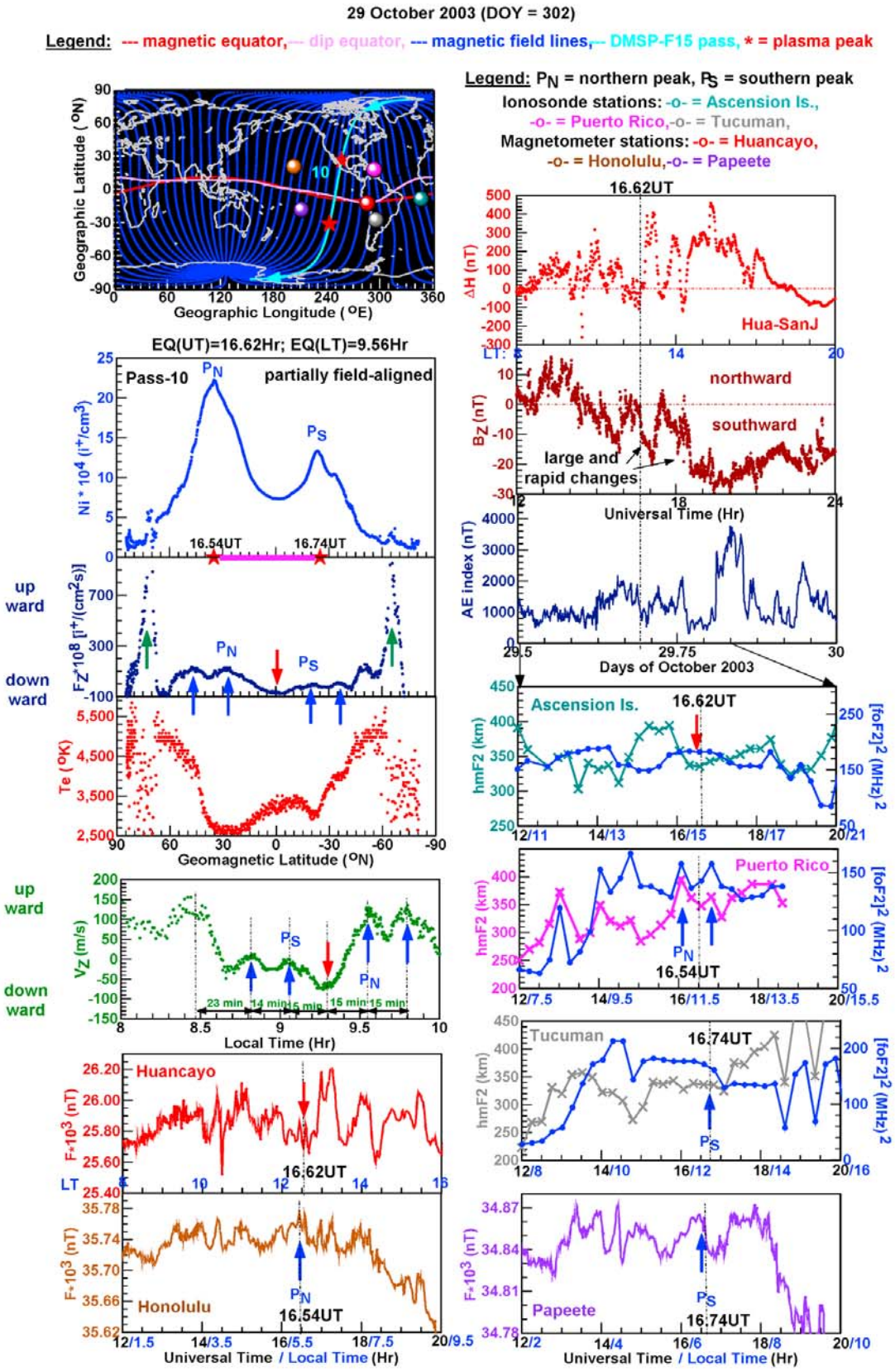

Figure 5. The same as for Figure 4, but for ~1630 UT.

over the African continent (see Figure 4) at an earlier UT (0800 UT), large-scale TIDs were still active at 1630 UT and created an EIA-like feature at ~0930 LT. The line plots of ΔH (derived from the local Huancayo-San Juan magnetometer data), IMF $\mathbf{B_Z}$ component, and AE index show periodic variations at ~1630 UT. These indicate that high-latitude energy injections triggered $\mathbf{E} \times \mathbf{B}$ drift fluctuations and launched TIDs. Again, we utilized ionosonde data to observe the TID-related upward and downward drift signatures. Measured at the nearby equatorial Ascension Island, the strong equatorial downward drift significantly lowered the maximum F2 layer height (from ~400 to ~330 km) and suppressed the increase of daytime plasma density. According to the Puerto Rico (close to the northern peak) and Tucuman (close to the southern peak) data, the TID-related upward drifts kept both the height and the plasma density high over Tucuman, and created sudden increases in these parameters over Puerto Rico. Similarly to Figure 4, the signature of equatorial downward drift was a well-defined decrease in the nearby Huancayo total **B**-field (F) data. Meanwhile, the nearby Honolulu and Papeete F-component data registered a well-defined increase at the northern and southern peak, respectively. These **B**-field signatures provide further observational evidence of the presence of large-scale TIDs (see details in section 3.2).

3.4. Temporal Variations of an EIA-Like Feature in the Local Morning Sector (1900 UT) on 30 October Over the Western Pacific

[21] To investigate how this EIA-like feature and the underlying large-scale TIDs varied in time, passes with early-morning LT recorded on 30 October over the Western Pacific were analyzed (see Figure 6). Crossing the equator at ~0630 LT (1845 UT), the F13 spacecraft made field-aligned detections and tracked the true plasma density profile of an EIA-like feature. Its distinctive features are a broad equatorial trough and broad peaks (~±30°N; geomagnetic). Soon after this in UT (1900 UT) but at a later LT (~0745 LT), the F14 spacecraft made a mostly field-aligned detection, and tracked a better developed EIA-like feature also showing a broad equatorial trough region and peaks around ±30°N. These two passes show the sudden intensification of this EIA-like feature in the early-morning hours. Both passes' F_Z plots tracked strong downward flows over the equator (see red arrows) and strong upward flows at the peaks (see blue arrow). These indicate the absence of forward fountain circulation and the presence of large-scale TIDs that were traveling from high-latitudes (see green arrows) equatorward. Plotted in LT, the V_Z plots show these large-scale TIDs. Their period of time, measured in LT, increased from 12 to 14 min (at ~0630 LT) to 18–20 min (at ~0745 LT). Indicating strong equatorward neutral wind actions, sometimes the V_Z minimum became reduced or completely diminished creating a broad maximum. According to the nearby Guam-Chichijima ΔH plot, the local equatorial $\mathbf{E} \times \mathbf{B}$ drift remained very close to zero between 0600 UT (1600 LT) and 1800 UT (0400 LT) indicating no forward fountain action. These EIA-like features were detected before a downward $\mathbf{E} \times \mathbf{B}$ drift surge (2000–2200 UT; 0600–0800 LT), when the IMF $\mathbf{B_Z}$ component turned southward. However, the IMF $\mathbf{B_Z}$ component experienced periodic variations (±20 nT; 1600–1800 UT) before its southward turning. As the simultaneously occurring periodic AE increases indicate, these $\mathbf{B_Z}$ variations were triggered by high-latitude energy injections that launched large-scale TIDs (see details in section 3.2). A TID-related downward drift (see red arrow) was tracked in the far away equatorial Jicamarca data showing the decrease of both the plasma density and the hmF2 (from 410 to 340 km). At distant northern midlatitudes, the Osan and Dyess (see blue arrow) ionosonde data show the signatures of large upward drifts. All these TID signatures indicate the presence of large-scale TIDs in other longitude sectors as well. In the local magnetometer data, a sudden decrease of total **B**-field intensity (F) was seen at the equatorial Guam when the equatorial downward drift occurred. Meanwhile, some sudden increases were registered at Honolulu and Papeete when the northern- and southern-plasma-peak-related upward drifts took place, respectively. These **B**-field observations provide further evidence of the presence of large-scale TIDs (see details in section 3.2).

3.5. Development of an EIA-Like Feature at Around Local Midday (2030 UT) on 30 October Over the Pacific

[22] Up to this stage of our study, we have identified some typical plasma density characteristics of an EIA-like feature created by large-scale TIDs, and some TID signatures in the ionosonde and magnetometer data. In order to further investigate the daytime ionosphere on 30 October, we turned to the TOPEX TEC, ionosonde, and magnetometer data. Crossing the equator at ~1100 LT, the descending TOPEX passes of cycle 409 provided mostly continuous TEC profiles over the Pacific and detected the first sudden development of an EIA-like feature at ~1100 LT (2030 UT) along pass 234. Figure 7 is constructed to illustrate the different aspects of this event. In order to demonstrate the strong similarities between the EIA-like features tracked by this TOPEX pass (234) and by the mostly field-aligned DMSP F15 pass (10) a day before (see Figure 5), the TEC and Ni line plots are shown together in geographic latitudes. Demonstrated in Figure 5, this EIA-like feature seen in the Ni data was created by large-scale TIDs (see details in section 3.3). Because of the closeness of these passes in the south (see map), the southern peaks are situated at similar latitudes (31.4°S tracked by F15 and 27.4°S estimated from the TOPEX TEC profile as there was a gap in the TOPEX data). Although the TOPEX pass is not field-aligned, it still provides a field-aligned-like TEC profile indicating that the sudden development of this EIA-like feature took place over a large geographic area and lasted for at least one UT hour. The strong similarities between the Ni and TEC profiles suggest that large-scale TIDs had a significant role in the development of this TOPEX detected EIA-like feature. This suggestion was confirmed by the ionosonde and magnetometer data only, as there were no F_Z data to track the underlying plasma circulation. In the nearby equatorial Jicamarca ionosonde data, a sudden decrease in height (from 410 to 310 km; see red arrow) and plasma density at ~20.5 UT (or 2030 UT) indicate a TID-related downward drift over the dip equator. On both sides of the Pacific, the Dyess and Osan ionosonde recorded at northern-peak-latitudes at 2021 UT (or 20.35 UT; see blue arrows) show the signatures of strong TID-related upward drifts. Because of the different local times, only the daytime

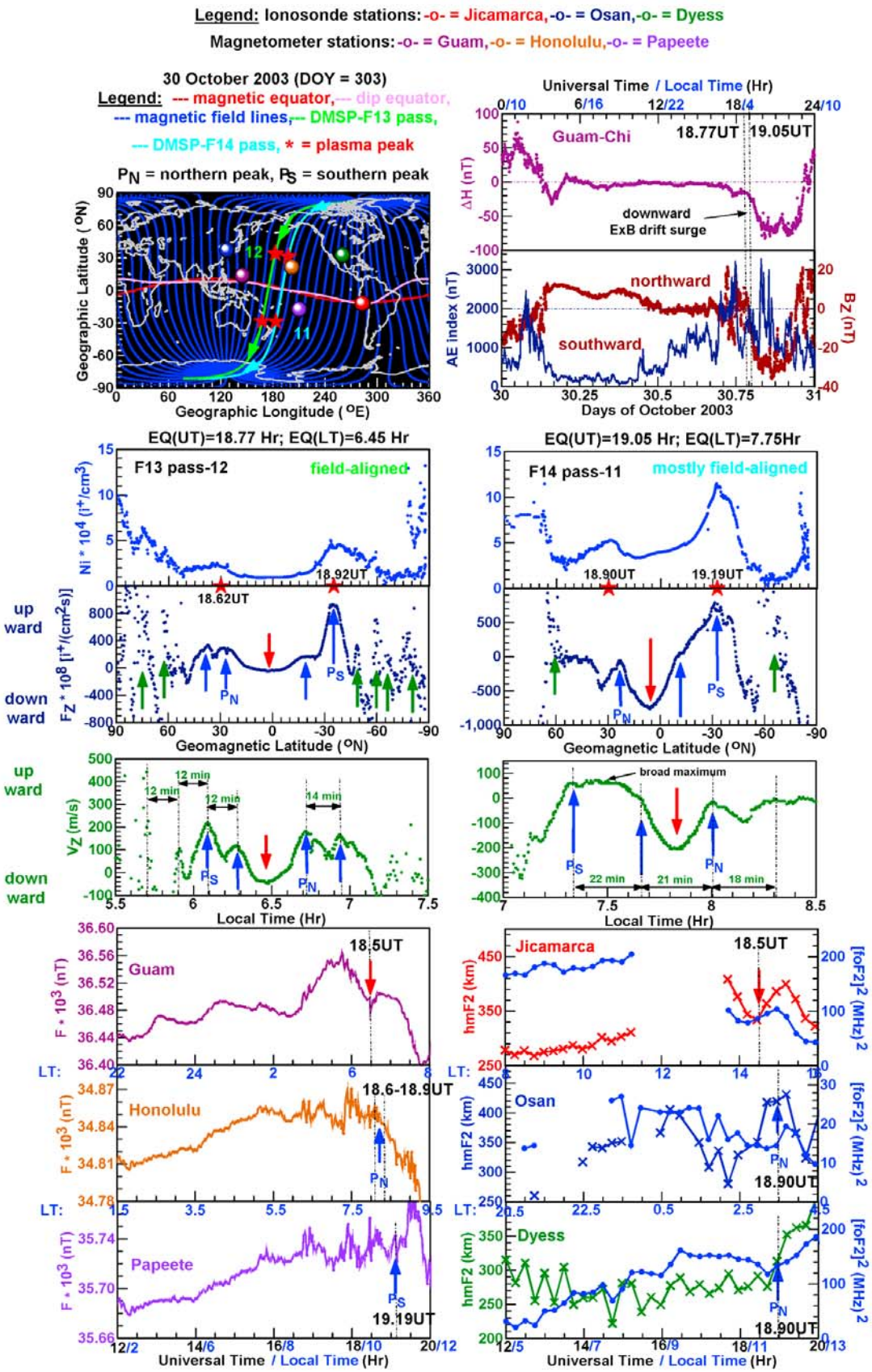

Figure 6. Two line plot sets show how an EIA-like feature, and its underlying large-scale TIDs and related TID signatures varied from ~0630 to ~0745 LT at ~1900 UT on 30 October 2003.

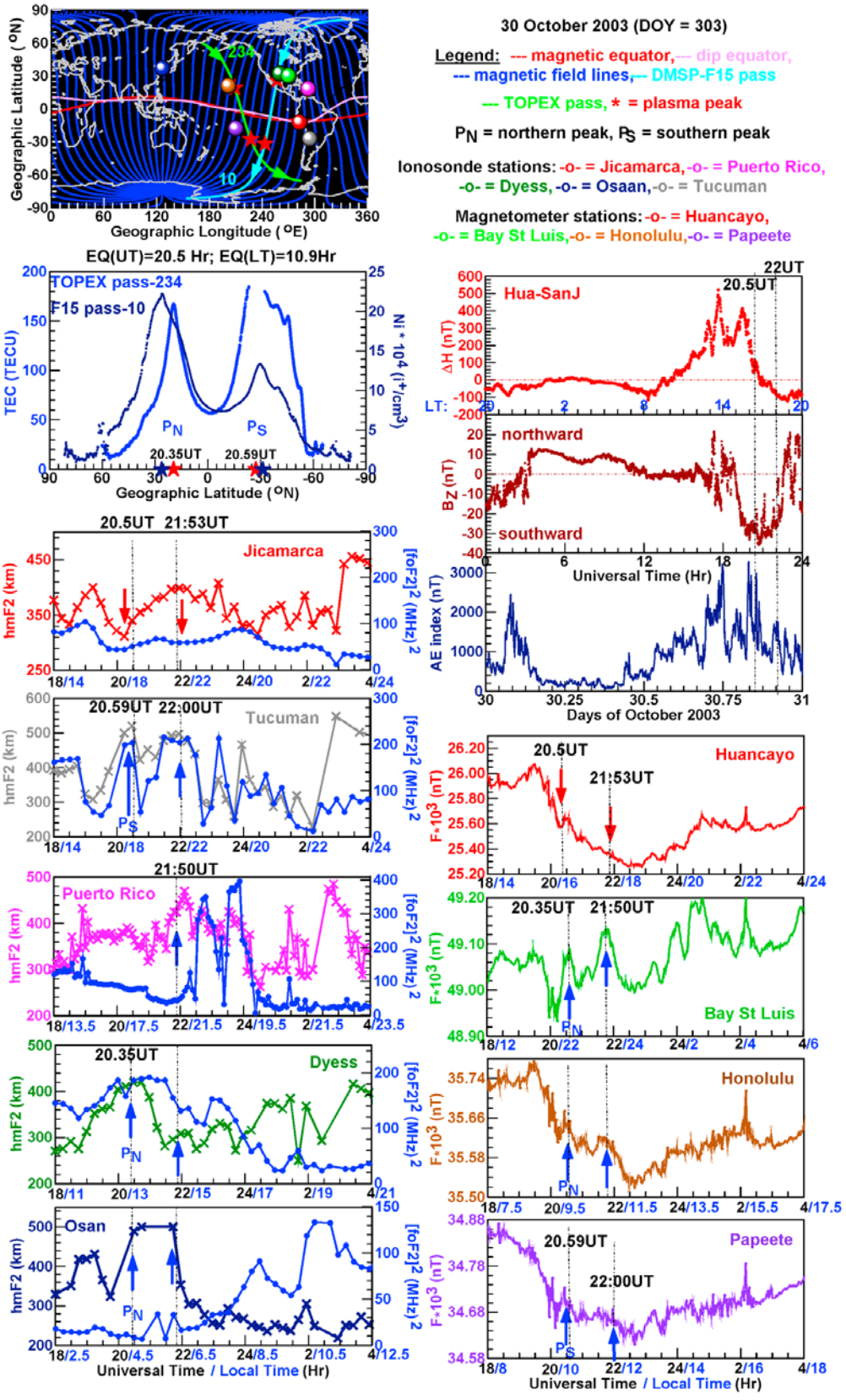

Figure 7. The TOPEX pass 234 show the TEC profile of the morning (~1100 LT) ionosphere at ~2000 UT on 30 October 2003. Ionosonde and magnetosphere data sets registered TID signatures indicating that the TOPEX pass tracked an EIA-like feature. At ~2200 UT, forward plasma fountain and TID signatures suggest a competition between the underlying physical mechanisms.

Dyess data (1300 LT) indicate an equally strong plasma density increase. Because of the early local morning hours (0500 LT), there was a minimal plasma density increase over Osan. At southern plasma-peak-latitude, the Tucuman data at local evening (1830 LT) show equally strong height and plasma density increases that are the signatures of a TID-related upward drift. According to the local Huancayo-San Juan ΔH data, the vertical $\mathbf{E} \times \mathbf{B}$ drift turned upward at 1400 UT (1000 LT) and reached its daytime maximum at 1800 UT (1400 LT). As indicated by the AE index, large energy injections took place during this time that created periodic $\mathbf{B_Z}$ variations and launched large-scale TIDs. Furthermore, well-defined TID signatures were observed in the magnetometer data recorded at Honolulu (at the northern peak), Bay St Luis (away from the northern peak), Papeete (at the southern peak), and at the equatorial Huancayo. All these observations indicate that large-scale TIDs created this EIA-like feature seen in the TOPEX TEC data.

4. Discussion

[23] We have demonstrated in Figures 4–6 the sudden development of EIA-like features in the early local morning hours (0800–0930 LT on 29–30 October 2003) of the Halloween Superstorm, these features' formation by large-scale TIDs and the crucial role of equatorward wind surges maintaining their high plasma densities. We have detected clean and regular periodic F_Z and V_Z variations indicating no sign of disturbance resulting from any forward fountain circulation. These findings contradict the results of *Batista et al.* [2006] regarding the sudden intensification of the EIA's southern crest on 29 October 2003 over South America. The development of an EIA is a gradual process that starts (at 0700 LT during quiet times) when the vertical $\mathbf{E} \times \mathbf{B}$ drift turns upward [*Fejer et al.*, 1995]. Our results suggest that during these early local morning hours (0800–0930 LT), the EIA had not been developed yet. If it just started developing, then any forward plasma fountain circulation was grossly over-ridden by large-scale TID-related vertical plasma flows. The accompanying strong equatorward wind surges were successfully reproduced by CTIP (see Figure 3) supporting the studies of *Lin et al.* [2005] and *Balan et al.* [2009] on the equatorward wind action that is essential for the development of positive storm effects.

[24] Shown in Figure 7, we have also demonstrated that the EIA-like feature tracked by TOPEX over the Eastern Pacific at 2030 UT (1100 LT) was created by large-scale TIDs. There are great similarities between this TOPEX TEC line plot and the CHAMP TEC line plot of *Mannucci et al.* [2005] shown in their Figure 3. Indicated in red, that CHAMP TEC plot depicts also a large EIA-like feature. It was tracked over the Eastern Pacific on 30 October along a non-field-aligned pass at similar UT and LT (2000 UT; 1230–1330 LT) than the EIA-like feature (2030 UT; 1100 LT) seen in the TOPEX data (see Figure 7 in this study). *Mannucci et al.* [2005] interpreted this CHAMP TEC profile as a large EIA contradicting this study's results regarding the absence of forward fountain action and the role of large-scale TIDs in its development. The results of *Ding et al.* [2007] show also the onset of large-scale TIDs at ~1850 UT on 30 October. Possibly, these large-scale TIDs were still operational at 2000 UT and destroyed an earlier developed (~1850 UT) regular equatorial anomaly (tracked by CHAMP; see dark blue line plot in Figure 3 of *Mannucci et al.* [2005]) by over-riding any forward fountain circulation. This assumption is supported by the ionosonde data plots in our study showing no forward fountain action over the dip equator and at midlatitudes at ~2000 UT. Thus, at that early stage of their investigation, the large midlatitude TEC enhancements (~210 TECU) appearing at 2000 UT were interpreted incorrectly as daytime superfountain effects by *Mannucci et al.* [2005] and *Tsurutani et al.* [2008].

[25] Another interesting feature of the 30 October 2003 events is the CHAMP detected EIA-like feature's (see red curve) further intensification at ~2200 UT (see black curve in Figure 3 of *Mannnucii et al.* [2005]). In order to identify long-wave TID signatures, we also marked the time of 2200 UT in the various line plots of Figure 7. According to the Jicamarca ionosonde data, there was a height rise over the dip equator (2153 UT) indicating forward fountain action but it was damped by a TID-related downward drift as the constant hmF2 values (400 km) and large plasma density depletion indicate. At the northern (2150 UT) and southern (2200 UT) crest, significant height increases were seen in the ionosonde data indicating TID-related upward drifts and equatorward neutral wind actions. Furthermore, long-wave TID signatures in the various magnetometer data were also seen at 2200 UT. These provide observational evidence that there was a competition between the large-scale-TID- and superfountain-related physical processes at 2200 UT. Thus, the large midlatitude TEC enhancements (270–325 TECU at ~2200 UT; see black curve in Figure 3 of *Mannnucii et al.* [2005]) were primarily due to large-scale-TID- and equatorward-wind-related upward drifts, and the superfountain effects were secondary.

5. Conclusions

[26] In this study, we have investigated plasma density features, which look like an EIA and therefore are called EIA-like features, occurring in the local early-morning hours of 29–30 October 2003 and at around local midday on 30 October. These are characterized by a broad equatorial trough and two peaks situated at ~±30°N (geomagnetic) suggesting forward superfountain circulation. Tracking their underlying plasma flow and vertical drift patterns in the DMSP data, we have unraveled the development of these EIA-like features. We have provided observational evidence that no forward superfountain circulation was present. Furthermore, we identified the signatures of large-scale TIDs and strong equatorial wind surges (successfully modeled by CTIP) in the DMSP data. Moreover, TID signatures were also identified in the ionosonde and magnetometer data. All these results provide observational evidence that these EIA-like features in the early-morning sector were created by TIDs and equatorward wind effects. Clear and undisturbed TID signatures seen in the ionosonde data indicate the absence of forward superfountain action in the development of the EIA-like feature at around local midday tracked by TOPEX (2000 UT; this study) and CHAMP (2030 UT; published results of *Mannucci et al.* [2005]). From our observational results we conclude that the strong

intensifications of low midlatitude plasma densities in the local morning sector of 29 and 30 October and at around local midday (~2000–2030 UT) on 30 October were due to the combined effects of large-scale TIDs and strong equatorward neutral winds, and not to the EIA as no forward fountain circulation was present. On the basis of the TID signatures observed in the ionosonde and magnetometer data, we also conclude that the high TEC detected (270–325 TECU; *Mannucci et al.* [2005]) over the Eastern Pacific at ~2200 UT was the result of a strong competition between the TID- and wind-related plasma flows, and the forward superfountain circulation. Long-scale TIDs and equatorward wind effects had primary importance, while forward superfountain effects were secondary.

[27] **Acknowledgments.** NICTA is funded by the Australian Government's Backing Australia's Ability initiative, in part through the Australian Research Council. We are thankful to the DMSP project teams for the data and to M. Hairston for his advice and gratefully acknowledge the US Air Force for providing the DMSP thermal plasma data. We are also thankful to JPL for the TOPEX radar data. The TOPEX data were obtained from the NASA Physical Oceanography Distributed Active Archive Center and the Jet Propulsion Laboratory/California Institute of Technology. We are grateful to the Community Coordinated Modeling Center for the CTIP model simulations. Simulation results have been provided by the Community Coordinated Modeling Center at Goddard Space Flight Center through their public Runs on Request system (http://ccmc.gsfc.nasa.gov). The CCMC is a multiagency partnership between NASA, AFMC, AFOSR, AFRL, AFWA, NOAA, NSF, and ONR. The CTIP model was developed by T. Fuller-Rowell at the Space Environment Center (NOAA SEC). We also thank the World Data Center for Geomagnetism at Kyoto (http://swdcwww.kugi.kyoto-u.ac.jp/index.html) for providing the Kp and *Dst* indices and magnetometer data and Space Physics Interactive Data Resource (SPIDR) for the ionosonde data (http://spidr.ngdc.noaa.gov/spidr/query.do?group=Iono&).

[28] Zuyin Pu thanks A. Danilov and Eduardo Araujo-Pradere for their assistance in evaluating this manuscript.

References

Abdu, M. A. (1997), Major phenomena of the equatorial ionosphere-thermosphere system under disturbed conditions, *J. Atmos. Sol. Terr. Phys.*, *59*, 1505–1519, doi:10.1016/S1364-6826(96)00152-6.

Abdu, M. A., I. S. Batista, A. J. Carrasco, and C. G. M. Brum (2005), South Atlantic magnetic anomaly ionization: A review and a new focus on electrodynamic effects in the equatorial ionosphere, *J. Atmos. Sol. Terr. Phys.*, *67*, 1643–1657, doi:10.1016/j.jastp.2005.01.014.

Abdu, M. A., et al. (2008), Abnormal evening vertical plasma drift and effects on ESF and EIA over Brazil-South Atlantic sector during the 30 October 2003 superstorm, *J. Geophys. Res.*, *113*, A07313, doi:10.1029/2007JA012844.

Afraimovich, E. L., S. V. Voeykov, and I. V. Zhivet'ev (2005), The ionosphere response to the sudden storm commencement on 29 October 2003 from GPS networks data, paper presented at the Proceedings of the URSI Ga, GP1G01.1(0246).

Afraimovich, E. L., S. V. Voeykov, N. P. Perevalova, and K. G. Ratovsky (2008), Large-scale traveling ionospheric disturbances of auroral origin according to the data of the GPS network and ionosondes, *Adv. Space Res.*, *42*, 1213–1217, doi:10.1016/j.asr.2007.11.023.

Balan, N., K. Shiokawa, Y. Otsuka, S. Watanabe, and G. J. Bailey (2009), Super plasma fountain and equatorial ionization anomaly during penetration electric field, *J. Geophys. Res.*, *114*, A03310, doi:10.1029/2008JA013768.

Basu, S., et al. (2001), Response of the equatorial ionosphere in the South Atlantic region to the great magnetic storm of July 15, 2000, *Geophys. Res. Lett.*, *28*, 3577–3580, doi:10.1029/2001GL013259.

Basu, S., Su. Basu, F. J. Rich, K. M. Groves, E. Mackenzie, C. Coker, Y. Sahai, P. R. Fagundes, and F. Becker-Guedes (2007), Response of the equatorial ionosphere at dusk to penetration electric fields during intense magnetic storms, *J. Geophys. Res.*, *112*, A08308, doi:10.1029/2006JA012192.

Batista, I. S., M. A. Abdu, J. R. Souza, F. Bertoni, M. T. Matsuoka, P. O. Camargo, and G. J. Bailey (2006), Unusual early morning development of the equatorial anomaly in the Brazilian sector during the Halloween magnetic storm, *J. Geophys. Res.*, *111*, A05307, doi:10.1029/2005JA011428.

Ding, F., W. Wan, B. Ning, and M. Wang (2007), Large-scale travelling ionospheric disturbances observed by GPS total electron content during the magnetic storm of 29–30 October 2003, *J. Geophys. Res.*, *112*, A06309, doi:10.1029/2006JA012013.

Fejer, B. G., E. R. de Paul, R. A. Heelis, and W. A. Hanson (1995), A global equatorial ionospheric vertical plasma drifts measured by the AE-E satellite, *J. Geophys. Res.*, *100*, 5769–5776, doi:10.1029/94JA03240.

Hocke, K., and K. Schlegel (1996), A review of atmospheric gravity waves and traveling ionospheric disturbances: 1982–1995, *Ann. Geophys.*, *14* (9), 917–940.

Horvath, I. (2006), A total electron content space weather study of the nighttime Weddell Sea Anomaly of 1996/1997 southern summer with TOPEX/Poseidon radar altimetry, *J. Geophys. Res.*, *111*, A12317, doi:10.1029/2006JA011679.

Horvath, I. (2007), Impact of 10 January 1997 geomagnetic storm on the nighttime Weddell Sea Anomaly: A study utilizing data provided by the TOPEX/Poseidon mission and the Defense Meteorological Satellite Program, and simulations generated by the Coupled Thermosphere/Ionosphere Plasmasphere model, *J. Geophys. Res.*, *112*, AO6329, doi:10.1029/2006JA012153.

Horvath, I., and B. C. Lovell (2008), Formation and evolution of the ionospheric plasma density shoulder and its relationship to the superfountain effects investigated during the 6 November 2001 great storm, *J. Geophys. Res.*, *113*, A12315, doi:10.1029/2008JA013153.

Horvath, I., and B. C. Lovell (2009), Distinctive plasma density features of the topside ionosphere and their electrodynamics investigated during southern winter, *J. Geophys. Res.*, *114*, A01304, doi:10.1029/2008JA013683.

Hunsucker, R. D. (1982), Atmospheric gravity waves generated in the high-latitude ionosphere: A review, *Rev. Geophys.*, *20*, 293–315, doi:10.1029/RG020i002p00293.

Kendall, P. C., and W. M. Pickering (1967), Magnetoplasma diffusion at F2-region altitudes, *Planet. Space Sci.*, *15*, 825–833, doi:10.1016/0032-0633(67)90118-3.

Lin, C. H., et al. (2005), Theoretical study of the low- and midlatitude ionospheric electron density enhancement during the October 2003 superstorm: Relative importance of the neutral wind and the electric field, *J. Geophys. Res.*, *110*, A12312, doi:10.1029/2005JA011304.

Mannucci, A. J., B. T. Tsurutani, B. A. Iijima, A. Komjathy, A. Saito, W. D. Gonzalez, F. L. Guarnieri, J. U. Kozyra, and A. Skoug (2005), Dayside global ionospheric response to the major interplanetary events of October 29–30, 2003 "Halloween Storms," *Geophys. Res. Lett.*, *32*, L12S02, doi:10.1029/2004GL021467.

Perevalova, N. P., E. L. Afraimovich, S. V. Voeykov and I. V. Zhivetiev (2008), Parameters of large-scale TEC disturbances during the strong magnetic storm on 29 October 2003, *J. Geophys. Res.*, *113*, A00A13, doi:10.1029/2008JA013137.

Prolss, G. W. (1987), Storm-induced changes in the thermospheric composition at middle latitudes, *Planet. Space Sci.*, *35*, 807–811, doi:10.1016/0032-0633(87)90041-9.

Rishbeth, H., T. J. Fuller-Rowell, and A. D. Rodger (1987), F-layer storms and thermospheric composition, *Phys. Scr.*, *36*, 327–336, doi:10.1088/0031-8949/36/2/024.

Sahai, Y., et al. (2005), Effects of the major geomagnetic storms of October 2003 on the equatorial and low-latitude F region in two longitude sectors, *J. Geophys. Res.*, *110*, A12S91, doi:10.1029/2004JA010999.

Tsurutani, B., et al. (2004), Global dayside ionospheric uplift and enhancement associated with interplanetary electric fields, *J. Geophys. Res.*, *109*, A08302, doi:10.1029/2003JA010342.

Tsurutani, B., et al. (2005), The October 28, 2003 extreme EUV solar flair and resultant extreme ionospheric events: Comparison to other Halloween events and the Bastille Day events, *Geophys. Res. Lett.*, *32*, L03S09, doi:10.1029/2004GL021475.

Tsurutani, B. T., et al. (2008), Prompt penetration electric fields (PPEFs) and their ionospheric effects during the great magnetic storm of 30–31 October 2003, *J. Geophys. Res.*, *113*, A05311, doi:10.1029/2007JA012879.

Zurbuchen, T. H., G. Gloeckler, F. Ipavich, J. Raines, C. W. Smith, and L. A. Fisk (2004), On the fast coronal mass ejections in October/November 2003: ACE-SWICS results, *Geophys. Res. Lett.*, *31*, L11805, doi:10.1029/2004GL019461.

I. Horvath and B. C. Lovell, Security and Surveillance, School of Information Technology and Electrical Engineering, University of Queensland, St. Lucia, Brisbane, Qld 4072, Australia. (ihorvath@itee.uq.edu.au)